

## I. INTRODUCTION

- MR cardiac imaging with tagging or displacement encoding (DENSE) affords the opportunity to measure myocardial strains non-invasively with high accuracy with enormous potential benefit to patients and researchers.<sup>1</sup>
- Clinical use of tagging is burdened by the manual extraction of the heart borders and locations of points along tags.
- The most accurate reconstruction methods utilize 3D measures of motion and modelling with high degrees of freedom.<sup>2</sup>
- We favor the use of a prolate-spheroidal coordinate system (PSCS) matched to the heart left-ventricular geometry to represent the modes of deformation in a compact and efficient mathematical framework.<sup>3,4</sup>

**OBJECTIVE** To develop a method for computing myocardial wall strains more efficiently by matching patient tagged images directly to virtual tagged images under deformation via PSCS modes of displacement. This eliminates the time-consuming additional step of semi-automatically detecting the tags or points along the tags.

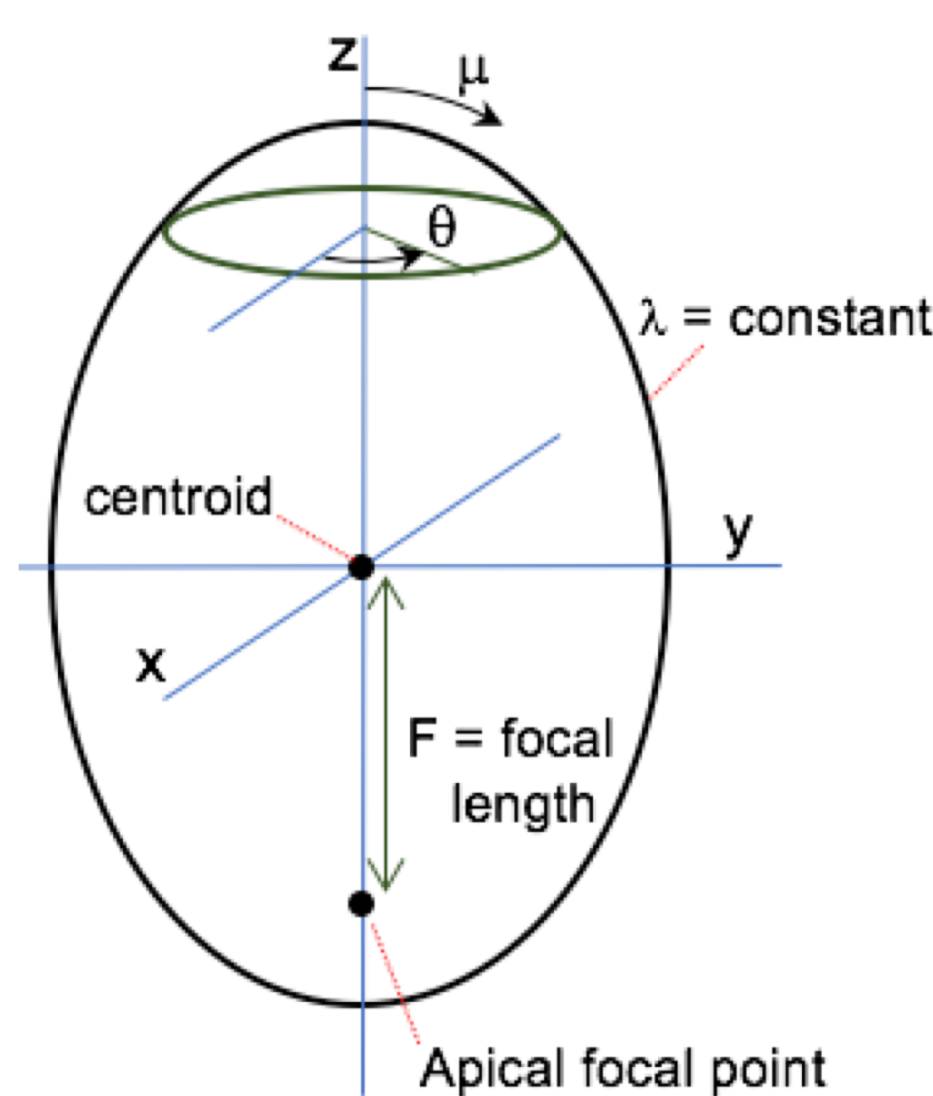
## II. METHODOLOGY

### MR IMAGE ACQUISITION

- General description: Any 3-D parallel or grid tagged cardiac MR images in long- and short-axis views, with 8-10 time points over the contraction (systolic) phase of the cardiac cycle. DENSE, and other acquisitions are also amenable.
- A low-quality human data set with sparse image/tag sampling and poor tag contrast was used to test robustness.

### DISPLACEMENT MODEL

- The motion of the heart left ventricle (LV) was defined by the modes of deformation in a local PSCS, followed by 6 bulk motions: 3 rotations followed by 3 translations. The modes are defined by the terms in the spherical harmonics series in the longitudinal and circumferential angles,  $\mu$  and  $\theta$ , and a power series in radial coordinate  $\lambda$ .
- The motion de-warps the heart from the follow-up time frame back to time 0 when the tags were generated. The local PSCS is defined in the follow-up time frame.



$$\Delta\lambda(\Delta\mu, \Delta\theta) = \sum_{n=0}^N \lambda^n \sum_{l=0}^L \sum_{m=-l}^l a_l P_l^{|m|}(\cos \mu) \cdot \begin{cases} \sin m\theta & m > 0 \\ \cos m\theta & m \leq 0 \end{cases}$$

### GENERATING VIRTUAL TAGGED IMAGES

- The tag pixel intensity profile was modelled as an inverse Gaussian with value 255 outside the tag and 0 at the trough.
- The tag profile, orientation, spacing and offset from the top left corner define a virtual 2-D tagged image at time 0.

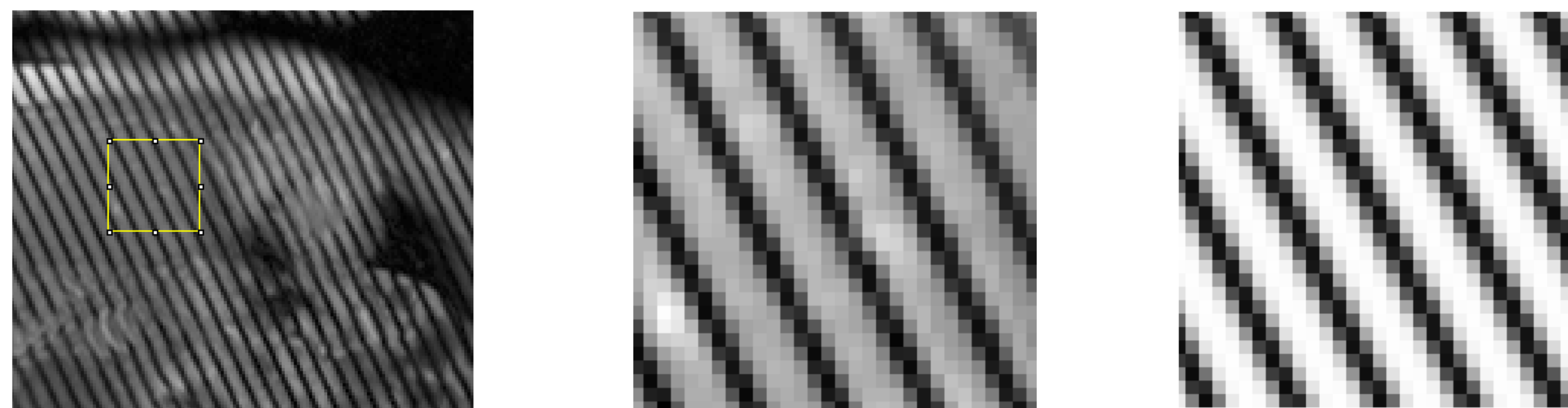


**Figure 2:** [A] depicts a liver region of interest (ROI: yellow box) in a patient short-axis image at time 0 (the heart is to the right of the ROI in this view). [B] shows the zoomed pixels within the ROI. [C] shows the virtual parallel-tag image generated optimized values for tag spacing, width, orientation and offset. Excellent agreement is achieved in the gray-scale pixel intensities across the set of tags.

### DETERMINING THE OPTIMAL DEFORMATION COEFFICIENTS

- Determine the local heart PSCS at the follow-up time from the semi-automatically segmented endocardial contours.
- Transform the voxel center locations to the local heart PSCS, then compute the  $\lambda$ ,  $\mu$  and  $\theta$  for these locations.
- Compute the displacements  $\Delta\lambda$ ,  $\Delta\mu$  and  $\Delta\theta$  at each voxel based on the current estimated coefficients  $a_{\lambda_i}$ ,  $a_{\mu_i}$  and  $a_{\theta_i}$ .
- Apply these to get the PS-based de-warping, and convert back to Cartesian coordinates (still in the local PSCS).
- Apply the bulk motions based on the current estimated rotations and translations in X, Y and Z.
- Transform back to scanner/world coordinates, and then into image slice in-plane coordinates (with sub-pixel precision).
- Compute the distance from this point to the nearest tag plane at time 0, and get the pixel intensity of this location.
- Do for all voxels to generate a virtual image at the follow-up time, and do for all slices in all series.
- Compute the normalized cross-correlation coefficient (NCCC) of the virtual image to the real MR image, over all slices.
- Iterate over all PS modes and bulk motions to achieve the highest NCCC match.

## ACKNOWLEDGEMENTS

Funding for this work is from the Ocala Royal Dames Foundation for Cancer Research and the Florida Department of Health Bankhead-Coley Cancer Research Program.

## III. RESULTS

### VIRTUAL TESTING DATA SET

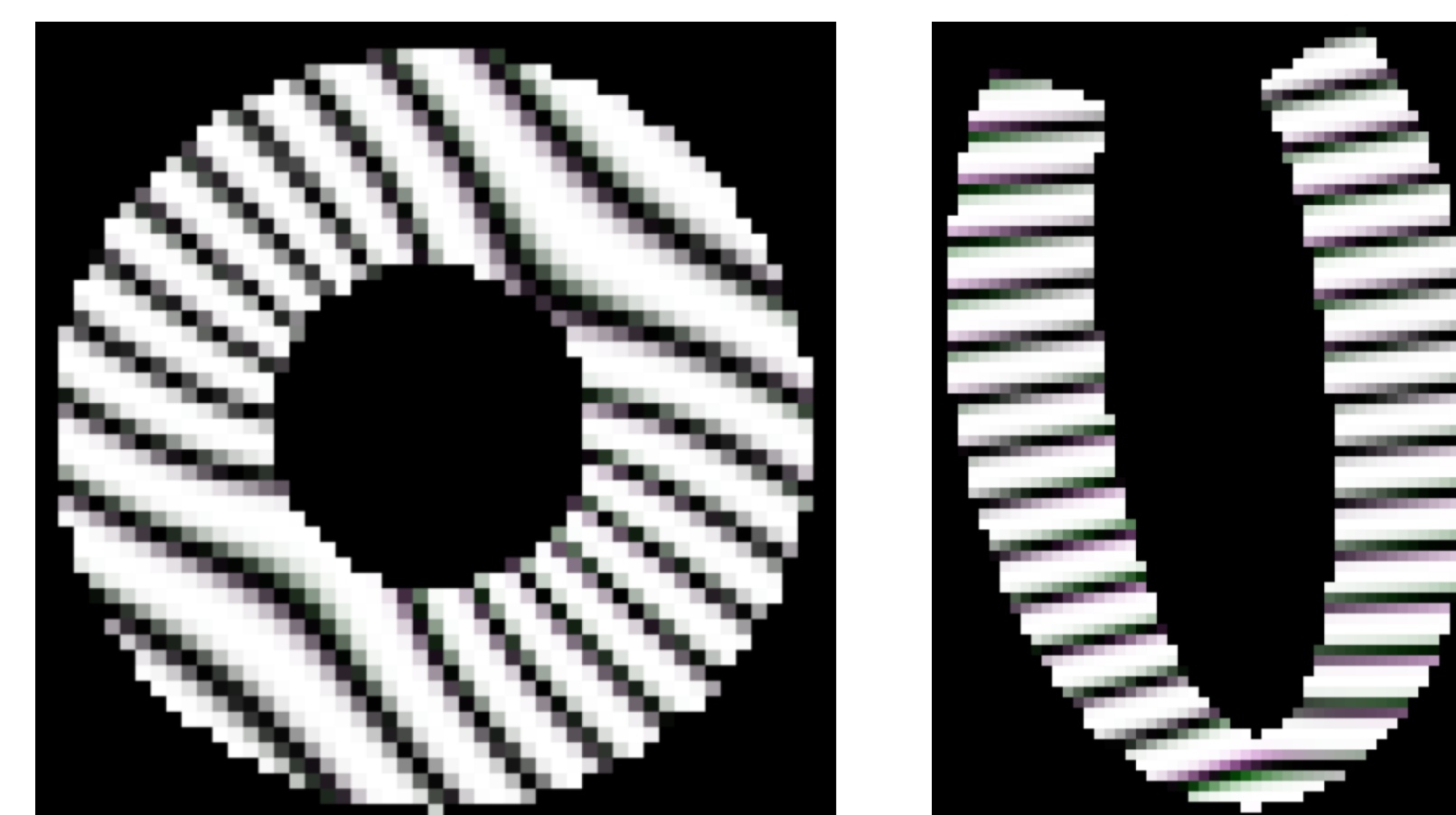


**Figure 3:** [A] and [B] show virtual tagged short- and long-axis images, respectively, at full contraction and with a colored overlay of the test deformation and the best-fit reconstructed images. Dark green highlights the tags in the testing images, pink highlights tags in the reconstructed images, and black/white results indicate exact alignment. [C] and [D] show radial strain (range 0.1 to 2.1) and strain error (-0.5 to 0.3).

**Table 1.** Point 3-D tracking, strains and errors. Given are the average magnitude and the standard deviation of the error between the mathematical ground-truth and the reconstructed estimates. The average strain value is given for comparison. The average strain values are greater than 7 times larger than the error standard deviation for all strains and mesh samples.

	All Points	Mid-wall only
3-D tracking error [mm]	0.2640	0.2422
3-D tracking error standard deviation [mm]	0.1977	0.1890
longitudinal strain error +/-	0.0011	0.0011
longitudinal strain error standard deviation	0.0072	0.0063
average longitudinal strain	-0.0493	-0.0485
circumferential strain error +/-	-0.0030	-0.0033
circumferential strain error standard deviation	0.0114	0.0108
average circumferential strain +/-	-0.2199	-0.2099
radial strain error +/-	-0.0137	-0.0121
radial strain error standard deviation	0.0617	0.0403
average radial strain value	0.5738	0.4456
thickness error +/-	0.0008	0.0011
thickness error standard deviation	0.0275	0.0178
average thickness +/-	0.4769	0.4019

### HUMAN DATA SET

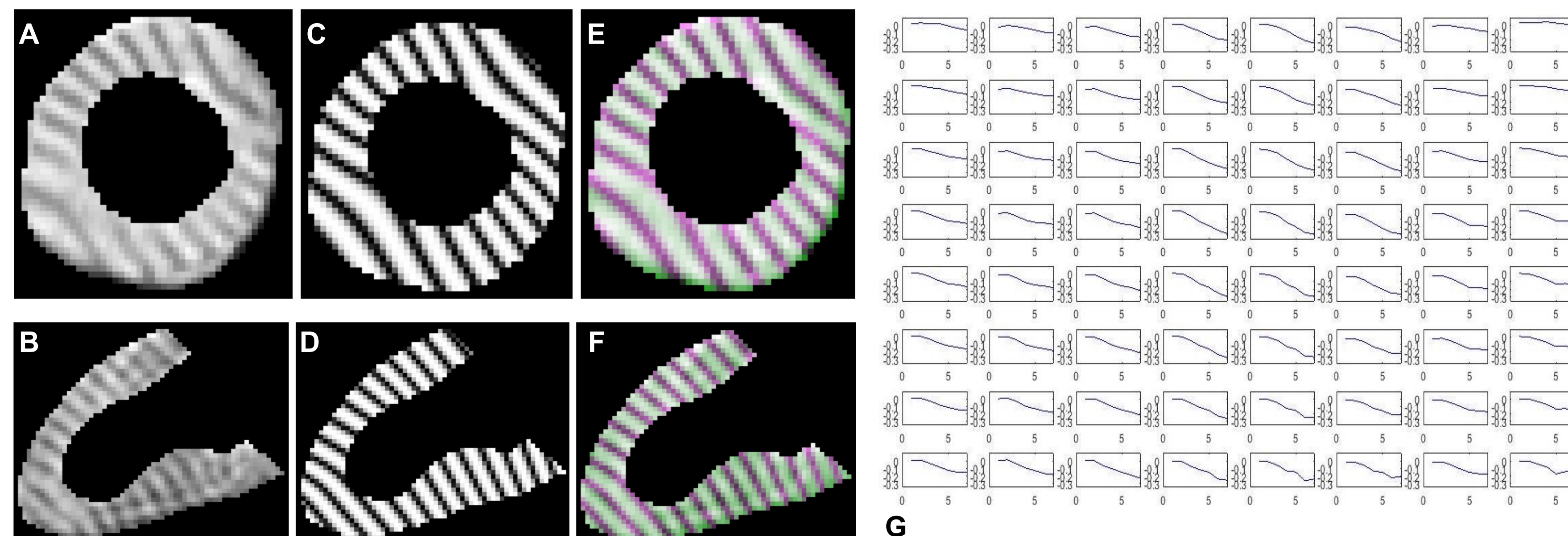


**Figure 4:** [A,B] show representative short- and long-axis human MR images cropped to myocardium at end-systole. [C, D] show the virtual tagged images at the same slice locations based on the reconstructed deformation with fitting order  $N=1$ ,  $L=2$ . [E, F] show the registration overlay. [G] shows a multi-plot of circumferential strain in the LV wall where the longitudinal level varies from the top row (more basal) to the bottom row (more apical) and left-to-right gives circumferential position starting at the mid-septum and wrapping to the LV free wall and back. Inside each box is plotted strain (vertical axis; range 0 to -0.3) versus time frame (range 0 to 7) at the mid-wall location.

## V. CONCLUSIONS AND DISCUSSION

An approach was developed to compute LV wall deformation directly from tagged MR images via generation of simulated tagged images and a 3-D model of heart deformation. This approach eliminates the laborious pre-processing step of detecting tags and/or points along tags, and of having to register two real MR scans. Our implementation employs an efficient and accurate representation of LV wall motion in terms of PSCS modes of deformation. The method was tested with a virtual test data set, and applied to a low-quality human image data set chosen to challenge robustness to sparse tag data and tag fading. The results show good reconstruction of the tag displacements in four dimensions, good handling of regions with poor tag quality, and has acceptable accuracy in point tracking and strains as quantified in the virtual test data set. It is hoped that this advancement will help accelerate application of quantitative MR tagging in the clinical and research arenas.

## VI. REFERENCES

- Ibrahim, E.-S. H. (2011). Myocardial tagging by cardiovascular magnetic resonance: evolution of techniques--pulse sequences, analysis algorithms, and applications. *Journal of Cardiovascular Magnetic Resonance: Official Journal of the Society for Cardiovascular Magnetic Resonance*, 13, 36.
- Declerck, J., Denney, T. S., Oztürk, C., O'Dell, W., & McVeigh, E. R. (2000). Left ventricular motion reconstruction from planar tagged MR images: a comparison. *Physics in Medicine and Biology*, 45(6), 1611-1632.
- O'Dell, W. G., Moore, C. C., Hunter, W. C., Zerhouni, E. A., & McVeigh, E. R. (1995). Three-dimensional myocardial deformations: calculation with displacement field fitting to tagged MR images. *Radiology*, 195(3), 829-835.
- O'Dell, W. G., & McCulloch, A. D. (2000). Imaging three-dimensional cardiac function. *Annual Review of Biomedical Engineering*, 2, 431-456. <https://doi.org/10.1146/annurev.bioeng.2.1.431>